

# Exo-C: A probe-scale space mission to directly image and spectroscopically characterize exoplanetary systems using an internal coronagraph

Karl R. Stapelfeldt<sup>a</sup>, Michael P. Brenner<sup>b</sup>, Keith R. Warfield<sup>b</sup>, Frank G. Dekens<sup>b</sup>,  
Ruslan Belikov<sup>c</sup>, Paul B. Brugarolas<sup>b</sup>, Geoffrey Bryden<sup>b</sup>, Kerri L. Cahoy<sup>d</sup>,  
Supriya Chakrabarti<sup>e</sup>, Serge Dubovitsky<sup>b</sup>, Robert T. Effinger<sup>b</sup>, Brian Hirsch<sup>b</sup>, Andrew Kissil<sup>b</sup>,  
John E. Krist<sup>b</sup>, Jared J. Lang<sup>b</sup>, Mark S. Marley<sup>c</sup>, Michael W. McElwain<sup>a</sup>,  
Victoria S. Meadows<sup>f</sup>, Joel Nissen<sup>b</sup>, Jeffrey M. Oseas<sup>b</sup>, Eugene Serabyn<sup>b</sup>,  
Eric Sunada<sup>b</sup>, John T. Trauger<sup>b</sup>, Stephen C. Unwin<sup>b</sup>

<sup>a</sup>NASA Goddard Space Flight Center, Code 667, Greenbelt MD 20771 USA

<sup>b</sup>Jet Propulsion Laboratory, California Institute of Technology, Pasadena CA 91109 USA

<sup>c</sup>NASA Ames Research Center, Moffet Field CA 94035

<sup>d</sup>Massachusetts Institute of Technology, Cambridge MA 02139

<sup>e</sup>Univ. of Massachusetts, Lowell MA 01854

<sup>f</sup>Univ. of Washington, Seattle WA 98195

## ABSTRACT

“Exo-C” is NASA’s first community study of a modest aperture space telescope designed for high contrast observations of exoplanetary systems. The mission will be capable of taking optical spectra of nearby exoplanets in reflected light, discover previously undetected planets, and imaging structure in a large sample of circumstellar disks. It will obtain unique science results on planets down to super-Earth sizes and serve as a technology pathfinder toward an eventual flagship-class mission to find and characterize habitable exoplanets. We present the mission/payload design and highlight steps to reduce mission cost/risk relative to previous mission concepts. At the study conclusion in 2015, NASA will evaluate it for potential development at the end of this decade.

**Keywords:** Exoplanets, high contrast imaging, optical astronomy, space mission concepts

## 1. INTRODUCTION

Over the past five decades, NASA has carried out ambitious space observatory projects designed to study the universe at new wavelengths with improved spatial resolution, spectral resolution, and field of view and with precise timing or photometry. In the 21st century, exoplanet research has emerged as a new focus for astrophysics and offers new space mission opportunities to explore. A new observational domain—imaging at very high contrasts and very small angular separations—must be opened if we are to understand the properties, formation, and evolution of planetary systems around stars like the Sun. The Exo-C probe mission study is an effort chartered by NASA HQ in 2013, with the goal of designing a modest-sized space observatory designed from the outset to meet the requirements of high contrast imaging, and to do so with a \$1 billion cost cap. It brings together a  $\sim 1.5$  m aperture, active wavefront control, internal coronagraphs with significant heritage in laboratory demonstrations, and a highly stable spacecraft environment to enable optical wavelength studies of nearby planetary systems at billion- to-one contrast. Exo-C will directly image and take spectra of planets beyond the reach of other telescopes. The mission and hardware design is patterned on the highly successful Kepler mission to achieve the same goal of delivering groundbreaking exoplanet science at an affordable cost.

The key enabling technology for Exo-C is a precision deformable mirror (DM) capable of being commanded and maintained at sub-angstrom accuracy. In conjunction with additional coronagraph elements to suppress

---

Further author information: (Send correspondence to K.R.S.)

K.R.S.: E-mail: karl.r.stapelfeldt@nasa.gov, Telephone: 1 301 286 3328

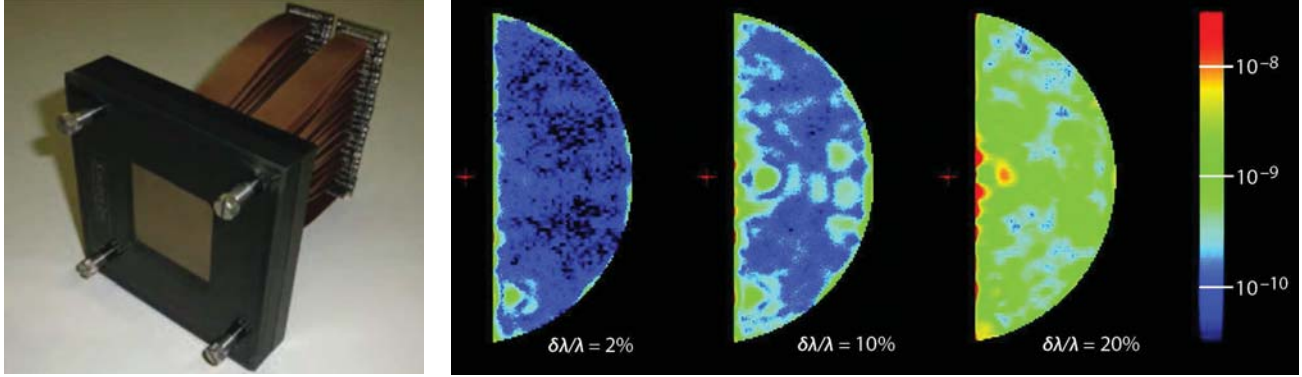


Figure 1. Exo-C Enabling Technology. Left: A Xinetics precision deformable mirror in 48x48 format. Right: High contrast dark fields created using a hybrid Lyot coronagraph and this deformable in a vacuum testbed at the Jet Propulsion Laboratory.

diffraction, the DM can be used to clear a high-contrast dark hole around the star out to a radius of  $N\lambda/2D$ , where  $N$  is the linear DM actuator count,  $\lambda$  is the wavelength, and  $D$  is the telescope aperture diameter. Laboratory demonstrations to date show that the needed level of  $10^{-9}$  contrast can now be achieved for unobscured pupils in a static system with optical bandwidths up to 20% (Fig. 1). Past exoplanet direct imaging mission concept studies utilizing this approach include ACCESS, EPIC, and PECO (Trauger et al. 2010; Clampin et al. 2010; Guyon et al. 2010). Exo-C brings previously competing groups together in an a single Science and Technology Definition Team supported by an Engineering Design Team at NASA/JPL. Technical readiness by 2017 and launch readiness in 2024 are required.

## 2. SCIENCE GOALS & REQUIREMENTS

Exo-C's prime science targets would be planetary systems within 20 pc of the sun. By the year Exo-C would launch, preceding ground and space telescopes have will identified stars hosting short-period transiting planets and gas giant planets on orbits  $\sim < 5$  AU. The atmospheric properties of hot, close-in planets will have been probed in the near-infrared by transit spectroscopy; and for hot, young planets by near-infrared adaptive optics imaging. While these advances will be remarkable scientific milestones, they will fall well short of the goal of obtaining images and spectra of planetary systems like our own. Exo-C would study cool planets in reflected light at visible wavelengths, ranging from gas giants down to super Earths, at separations from 1-9 AU, around nearby stars like the Sun.

### Science Requirements

Primary mirror diameter	$> 1.3$ m
Raw speckle contrast	$1e-09$
Contrast stability after control	$1e-10$
Spectral coverage	450-1000 nm
Inner working angle	$2\lambda/D = 0.22''$ @800 nm
Outer working angle	$> 20\lambda/D = 2''$ @800 nm
Spillover light from binary companion	$\leq 1e-9$ contrast @8''
Spectral resolution	$R \sim 70$
Astrometric precision	$< 30$ milliarcsec
Imaging camera field of view	1 arcminute
Integral Field Spectrograph field of view	$> 2''$
Mission lifetime	3 years

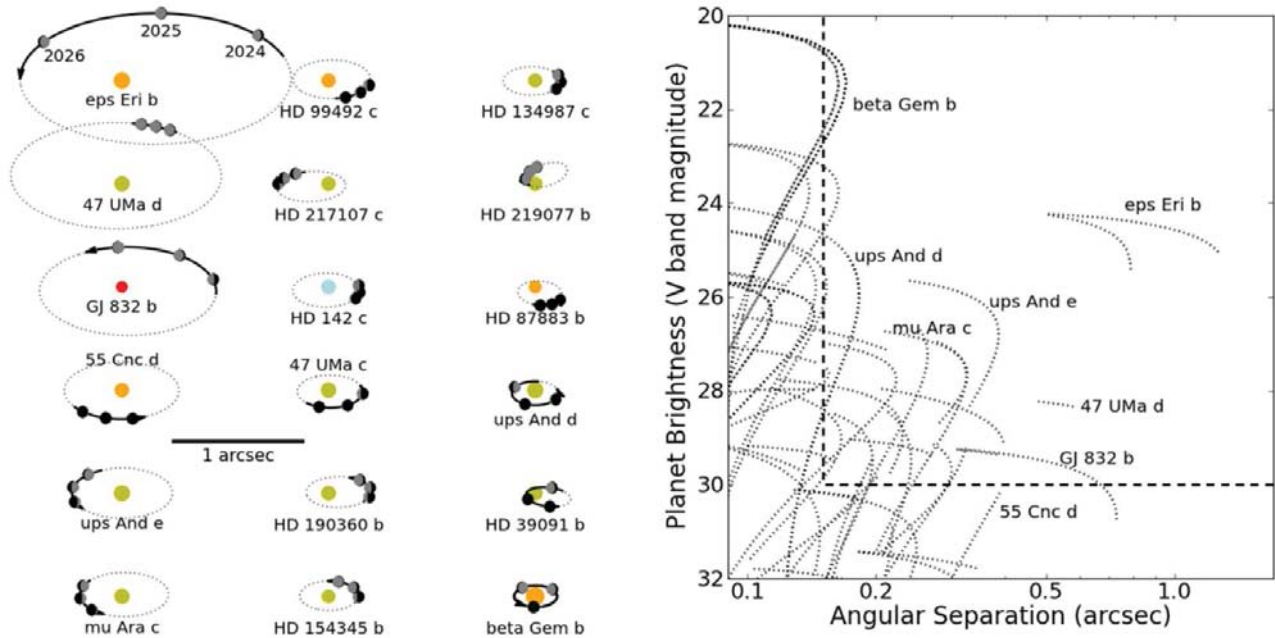


Figure 2. Known Planetary Targets. Exo-C will observe several known exoplanets whose orbital radius and orbital phase will be known during each observing epoch. Assuming an inclination of  $70^\circ$ , the illumination of the widest-separation/brightest planets is shown for three epochs from 2024 to 2026 (left panel). The brightness of each planet is shown as a function of orbital separation over the same time period (right panel). Targets must have sufficient angular separation ( $\geq 0.15''$ ) and must be bright enough ( $< 30$  mag) to be detected.

## 2.1 Exoplanet Spectra

Radial velocity (RV) surveys have detected many exoplanets around nearby stars, several of which are prime targets for Exo-C imaging. Beyond simply knowing that a planet is present, RV detections also determine the orbital separation and relative illumination as a function of time, such that an optimal epoch for observation can be chosen within the observatory lifetime. RV measurements also constrain the planet mass, particularly when the orbital inclination is determined by direct imaging, which aids in subsequent interpretation of the optical spectra. The RV planets orbit mature, quiet stars for which excellent elemental abundances can be derived. This will allow meaningful comparison of abundances measured in the planetary atmospheres to those of the star. As seen in Figure 2 ~ a dozen known RV planets have large enough angular separation and are bright enough for Exo-C to image. With the instrument inner working angle (IWA) increasing with wavelength, a full spectrum from 0.45–1.0  $\mu\text{m}$  can be obtained for about half of these planets.

The spectral range 450-1000 nm encompasses many molecular absorption bands of varying strengths of methane, water, and ammonia. The long wavelength cutoff is chosen to allow some detection of continuum on the red side of the 940 nm water band and the short wavelength cutoff is motivated by the relatively bland Rayleigh and haze-scattering spectrum expected in the blue for giant planets.

For spectral characterization, a spectral resolution of  $R = 70$  was chosen as the minimum required to detect and characterize methane bands with a variety of strengths, as well as the water band at 940 nm for Jovian planets. Additionally,  $R = 70$  is optimal for detecting the  $\text{O}_2$  A-band at 760 nm, a potential biosignature, should a super-Earth planet be found in the habitable zone of one of the stars in the alpha Centauri system. A signal to noise of 10 would be adequate for the measurement of these features.

## 2.2 Exoplanet Discovery Surveys

RV surveys are incomplete for orbital periods  $> 12$  years, for early F and hotter stars lacking strong metallic lines in their spectra, for stars with high chromospheric activity, and for planets in nearly face-on orbits. Multi-epoch

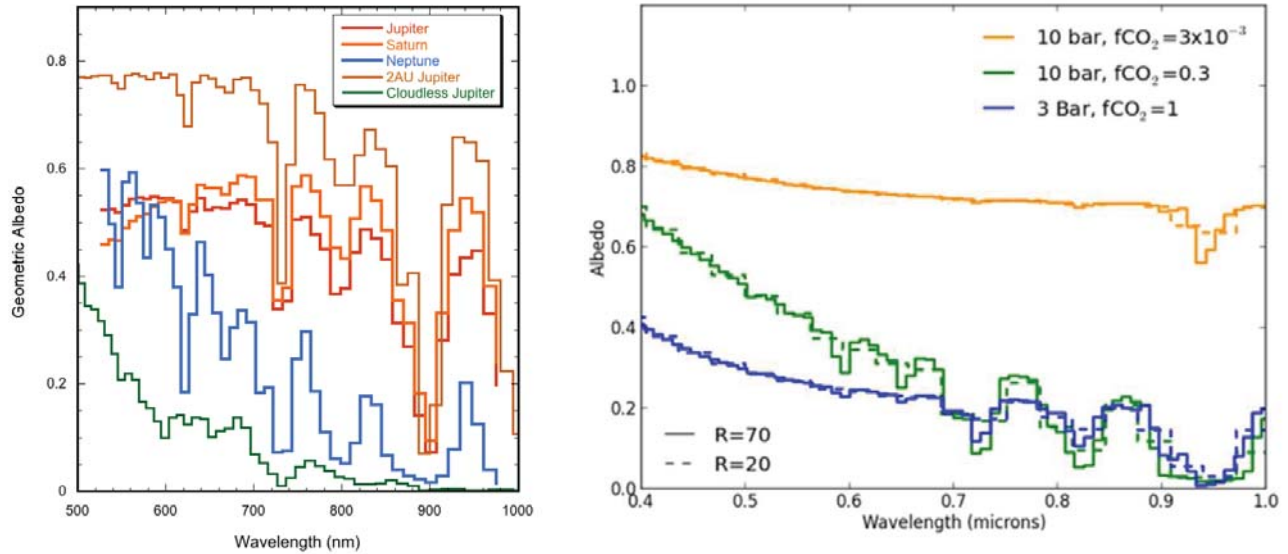


Figure 3. Example Target Spectra. Left: Geometric albedo spectra of real and model giant planets convolved to  $R = 70$  spectral resolution. Shown are Jupiter, Saturn, and Neptune (all from Karkoschka 1999), along with a warm Jupiter and a cloudless Jupiter three times enhanced in heavy elements from Cahoy et al. 2010. The warm Jupiter is very bright, while conversely the cloudless Jupiter is extremely dark. Right: Simulated spectra of super-Earth atmospheres with different total pressures and amounts of  $\text{CO}_2$  and water vapor.

imaging with Exo-Cs coronagraph has the potential to discover planets beyond RV limits around as many as 200 nearby stars (Fig. 2.2). There are more than 70 stars within 25 pc that host close-in RV planets and would be prime targets for outer planet searches. Exo-Cs contrast capability will permit detections of Jupiter-like planets on orbits out to 9 AU, Neptune-like planets out to 3 AU, 2 R mini-Neptunes out to 1.5 AU, and super-Earths at 1 AU. Particularly important survey targets will be the two Sun-like stars of the alpha Centauri binary system, the Sun's nearest neighbor. Spectral characterization of the brightest planet discoveries would be carried out. If Exo-C proves to be exceptionally stable and exozodiacal dust levels are low, photometric detection of Earth-sized planets would be possible in a handful of the nearest stars.

### 2.3 Disk Imaging

Debris disks trace the dust liberated by ongoing collisions in belts of asteroidal and cometary parent bodies. In addition to revealing the location of these belts, debris dust serves as a tracer of the dynamical signature of unseen planets. Exo-C will be capable of resolving rings, gaps, warps, and asymmetries driven by planetary perturbations in these disks. With contrast improved 1000 $\times$  over the Hubble Space Telescope (HST), Exo-C will be sensitive enough to detect disks as tenuous as our own Kuiper Belt, enabling comparative studies of dust inventory and properties across stellar ages and spectral types. Several hundred debris disk targets will be surveyed, including nearby stars with far-IR excess and RV planet systems where sculpted dust features might be seen. A smaller survey of young protoplanetary disks will reveal how small dust particles are distributed with respect to the larger particles traced by Atacama Large Millimeter/submillimeter Array (ALMA) imaging.

Exo-Cs inner working angle of  $0.15''$  at 550 nm is sufficient to spatially resolve the habitable zones of 10 Sun-like stars and another 40 stars with earlier spectral types. A survey of these targets will search for extended surface brightness from exozodiacal dust, to limits within a factor of 510 of the dust levels found in our own Solar System. The detected surface brightness will constrain the dust inventory and albedo, thus helping to define the background levels against which future missions will observe Earth-like extrasolar planets. In the nearest examples, Exo-C images may show asymmetric structures indicative of planetary perturbations to the dust distribution.

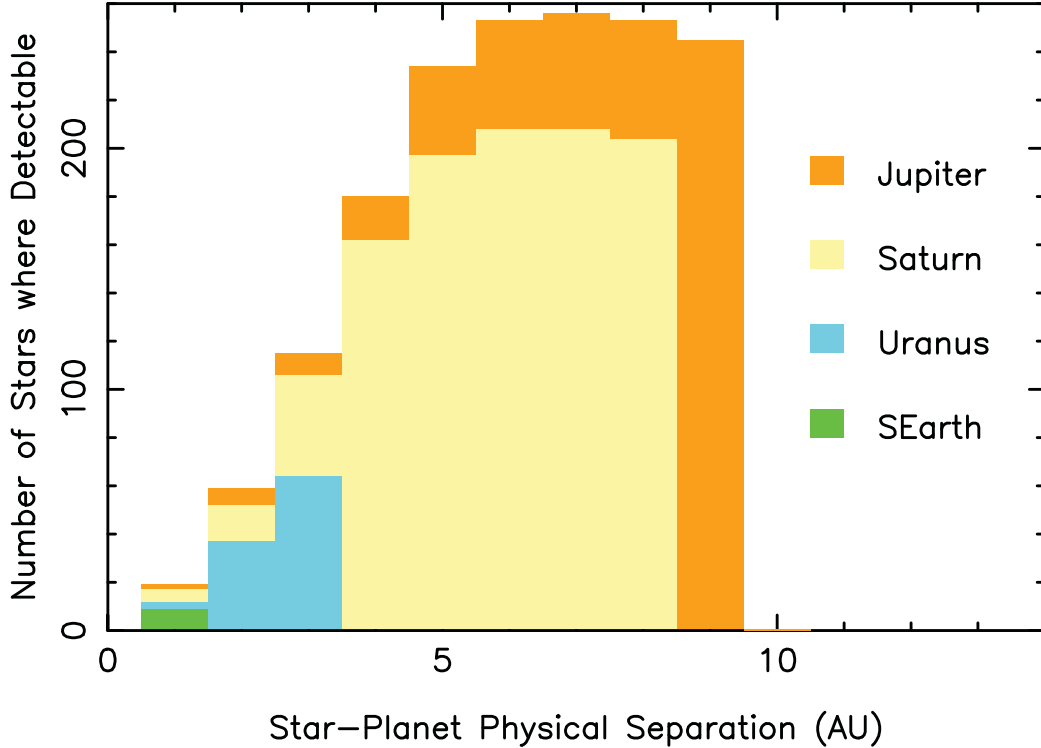


Figure 4. Exo-C Planet Search Space. These four histograms show the number of nearby Hipparcos stars where planets of various sizes and orbital radii can be detected in two visits and within a cutoff integration time. Due to the  $1/r^2$  law, smaller planets must be located closer to the star to be detected at the same fiducial contrast level of  $10^{-9}$ . The left side of these distributions is largely defined by Exo-C’s inner working angle, while the right side is defined by a limiting contrast of  $3 \times 10^{-10}$  derived from telescope stability considerations.

## 2.4 General Astrophysics

Exo-C’s imaging camera will carry a small filter set that will enable optical imaging and photometry of any astronomical target over its modest field of view. This could include temporal studies of solar system objects, if the project budget allowed the pointing system to be upgraded to track moving targets. The coronagraph could be utilized to study dust shells around post-main sequence objects and the host galaxies of quasars or AGN. Exo-C’s optical bench has sufficient volume to accommodate a second instrument and the payload mass budget would also allow this. The costs of a second instrument would require additional funds above the current \$1 B cost cap.

## 3. ARCHITECTURE TRADES

### 3.1 Telescope Type and Aperture

From a performance perspective, the use of an unobscured telescope form for a coronagraph is preferred. The two main factors involved in determining this were collecting area and integration time, both of which significantly favored the unobscured form. Five other factors were examined (polarization influence, fabrication complexity, structural considerations, optical design complexity, and binary target performance) that either yielded no net distinction or only very weakly favored one form over the other.

The science performance clearly increases with aperture size, since it increases the light collected. More important, the clear aperture size for a coronagraph sets the inner working angle (IWA). This in turn directly affects the number of known radial velocity (RV) exoplanets for which Exo-C is able to obtain spectra, and the number of Super-Earths that Exo-C would be capable of detecting. For the known RV planets shown in Fig. 2,

a 1.5m aperture provides sufficient IWA to make spectra of 10 targets out to  $\lambda = 800$  nm and could image 2  $R_e$  super-Earth targets if they are present around 10 other stars near the sun. A 1.4m aperture provides virtually the same performance, while a noticeable degradation is seen for a 1.3m aperture. All three aperture sizes appear feasible from a mass perspective for our assumed intermediate class launch vehicle, while cost considerations set 1.5m as the maximum size likely to be afforded given the \$1 B cost cap. 1.5m was thus selected as the aperture size for the Exo-C interim design work.

### 3.2 Orbit and Telescope Stability

Thermal stability of the telescope is a prime consideration for achieving the stable optical wavefronts needed for  $1e-09$  contrast imaging. Earth orbits (LEO, sun-synchronous, GEO) were not considered because the varying radiative inputs on the telescope could require complex countermeasures to control. L2 and Earth-trailing orbits provide the most benign thermal environments. These two options were compared in the areas of science capability (a function of sky accessibility and target availability) and a model-based cost estimation to determine engineering and operation cost differences to access and maintain the two orbits. Initial examination of this trade showed no significant target availability or data return advantage for Exo-C in L2 orbit over an Earth-trailing spacecraft. As a result, the major driver for orbit selection was the overall mission cost. Due to the need to carry extra propulsion capability for orbit maintenance and the need for a navigation team to execute that maintenance, L2 orbit would entail additional costs that the Earth-trailing orbit does not. Therefore, the Earth-trailing orbit was selected as the baseline orbit for the Exo-C Probe study.

In addition to choosing a stable orbit, body-fixed solar arrays and high-gain antenna were selected over articulated ones. This results in a stiffer observatory that will be less susceptible to dynamic excitation during slews or reaction wheel desaturations, and thus better pointing stability should be achieved. These choices are the same as those made by the Kepler mission to achieve their renowned photometric stability.

### 3.3 Science Instrument

There are three areas where options were considered: science image path, fine guidance sensor path, and spectrometer path. While a great many options could be implemented single architecture needed to be identified for the interim design. It is desirable to maximize the number of common elements between these three optical paths so that a common wavefront control system can be used for all three. An important constraint is that spectral coverage must be obtained piecewise in 20% wide bands, as this is the current state of the art for high contrast wavefront control. Doing this simultaneously in adjacent wavelength channels would require an excessively complex instrument - essentially four separate coronagraphs with their own pairs of deformable mirrors.

A single-path instrument with selectable elements (to provide coverage over the full waveband) was baselined. The fine guidance sensor (FGS) sees the light of the bright target star reflected off the coronagraphic mask and senses the pointing jitter at high rates. This signal can then be used to drive a fine-steering mirror (FSM) that keeps the star centered on the coronagraphic mask with no loss of signal to the science path. Broadband imaging is carried out with the science camera with different DM settings for each band. Spectroscopy is carried out with an integral field spectrometer (IFS) that shares the science field of view with the imaging camera, with a flip mirror to switch the input beam between the two. Implementation of an IFS has significant mission benefits. Its detector could perform as a reduced-capacity backup in the event of a failure of the imaging detector. It provides spectral diversity information of the residual speckle pattern, which will facilitate the derivation of wavefront control solutions, post-processing of the spectral images isolate planetary spectra from speckles, and the simultaneous spectroscopy of multiple planets and dust structures in the exoplanetary system.

Two basic configurations were examined to accommodate the coronagraph instrument. A lateral configuration, which places the instrument parallel and offset to the telescope axis, was selected for its ability to fulfill all desired functions while providing for best overall performance with a minimum total count and lowest angles of incidence on critical optical surfaces. This design is unique relative to the Hubble Space Telescope instruments, all of which were mounted behind the on-axis Cassegrain mirror. In a modest-size telescope like Exo-C, the lateral instrument bench provides more available room and better isolates the instrument from variable solar flux inputs during telescope pitch maneuvers.

### 3.4 Coronagraph Type

Five separate coronagraph architectures were considered: Hybrid Lyot (Trauger et al. 2012), Phase-Induced Amplitude Apodization (PIAA; Guyon et al. 2012), Shaped Pupils (Carlotti et al. 2012), Vector Vortex (Mawet et al. 2011), and the Visible Nuller (Lyon et al., 2012). Optical performance simulations were developed with design inputs from the architecture advocates, and implemented in a common software environment. These simulations included the effects of pointing jitter which degrades contrast performance and the inner working angle. The simulations were input to codes that calculated integration times for spectroscopy of known RV planets through each coronagraph type.

The results showed that (within the uncertainties) four of the five coronagraph types would produce similar science yields in the Exo-C observatory. The Shaped Pupil, by virtue of its larger inner working angle of  $3 \lambda/D$ , produced a significantly lower science yield and was thus eliminated from consideration for Exo-C. Following the Fall 2013 AFTA Coronagraph working group evaluations, the Visible Nuller was judged to be too technically immature for readiness in 2017 and was also dropped. The Hybrid Lyot coronagraph was chosen as the interim baseline for Exo-C on the basis of its superior contrast and bandwidth performance to date in the laboratory (Lawson et al. 2013), while the PIAA and Vector Vortex are being carried forward to a second round of evaluations.

## 4. BASELINE DESIGN

### 4.1 Mechanical

Exo-C has gravitated toward a Kepler-like design due to similar stability, aperture, and mission life requirements. With a total mission cost around \$750M FY15 - well below the Probe study \$1B requirement - Kepler makes an excellent starting point for the Exo-C design. Aside from the payload, Exo-C is very similar to Kepler in design, only needing to add a two-stage passive vibration isolation system to the original Kepler architecture. These passive isolators are flight proven technology. The only other planned changes to the bus are more reliable reaction wheels and some structural panel resizing.

Exo-C consists of the instrument payload attached to the spacecraft bus, as seen in Figure 5. Mounted directly to the top surface of the bus is the outer barrel assembly, which is comprised of the outer barrel structure and the outer lid. The outer barrel assembly encloses the payload, which includes the inner barrel assembly, the primary and secondary mirror assemblies, the primary support structure (PSS), the instrument bench with instruments and optics, the payload avionics, and the star trackers. Two openings in the outer barrel give the payload radiators a view to cold space. Both the inner and outer barrels have a scarfed baffle structure at the top. Along the height of the inner barrel are thin cylindrical ribs to suppress stray light. Mounted atop the PSS is the primary mirror assembly. The payload avionics are mounted to the underside of the PSS. The secondary mirror assembly is attached to the top of the inner barrel. The assembly is comprised of the secondary mirror, and the secondary support structure. The instrument bench is designed such that the optics and instruments are enclosed within the bench. Access holes have been designed into the top panel to enable installation and adjustment of the bench components. The payload is attached to the spacecraft bus at the PSS via a vibration isolation system to isolate the payload from bus disturbances. The payload contains two separate radiator panels. The instrument radiator panel attaches directly to the top instrument bench panel, while the payload avionics radiator mounts to the side of the PSS. Two star trackers, along with the star tracker electronics, attach to the inner barrel in between the instrument bench and the PSS. The star tracker electronics share a radiator with the payload electronics.

### 4.2 Thermal

The heliocentric, Earth-trailing orbit baselined for Exo-C is associated with extremely small planetary-based thermal loads, and the thermal design focuses on minimizing disturbances from varying incident solar loads. This is accomplished through the outer barrel assembly, which serves as a solar radiation shield. The outer diameter is covered with multi-layer insulation. The external layer minimizes solar absorption and resulting temperature increases. The inner diameter is also covered with multi-layer insulation. The inner barrel assembly serves as the secondary metering structure. It is actively temperature controlled to maintain its dimensional

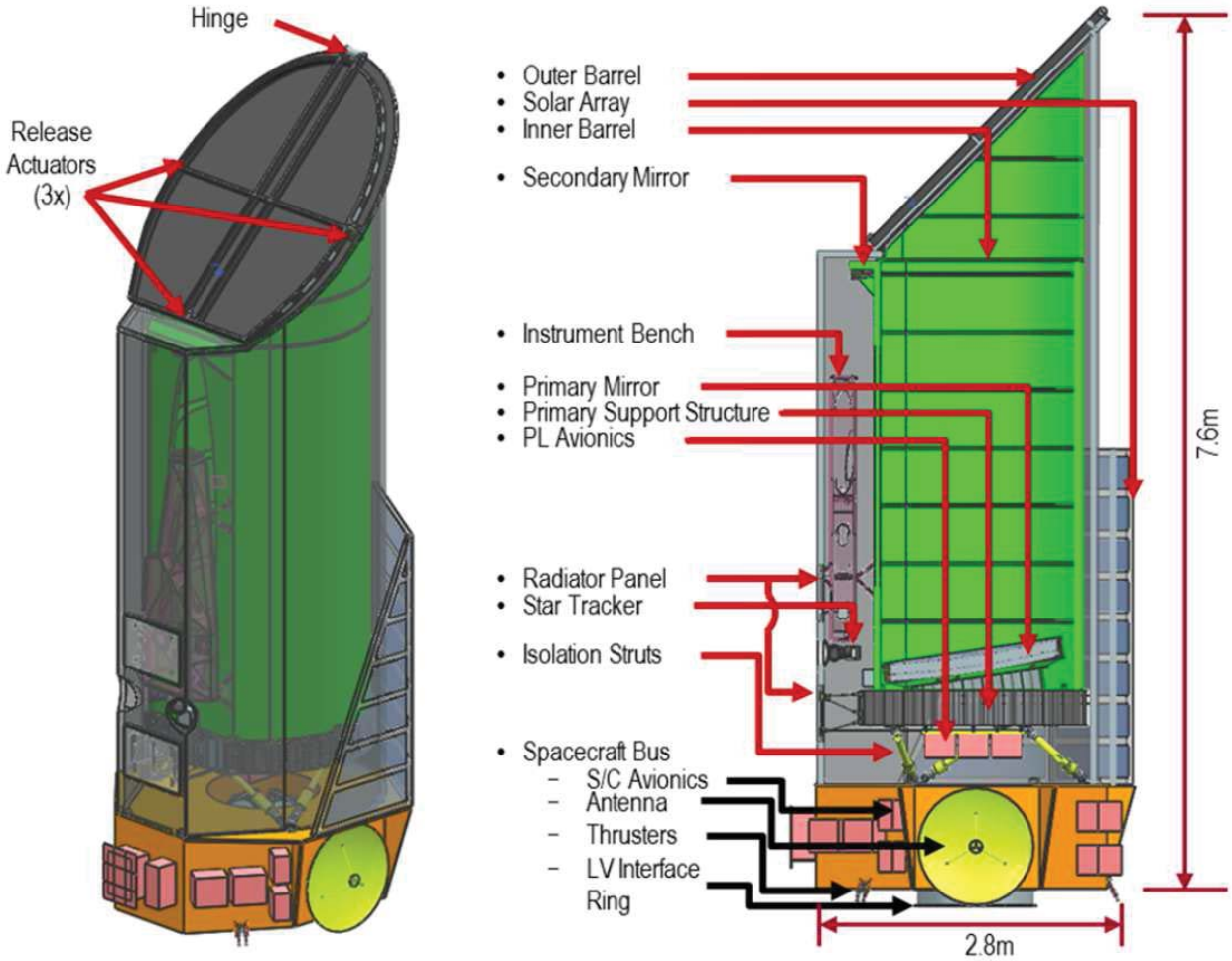


Figure 5. Interim Exo-C Observatory Configuration as of the interim study report.

stability and to provide a more constant temperature environment for the primary and secondary mirror surfaces, when subjected to varying solar incidence angles. Atop both barrel assemblies is a scarfed solar shield to allow up to 45° off-Sun pointing. Active heater control is also employed through radiative heating of the primary and secondary mirrors to reduce wavefront drift errors to acceptable levels within settling times of a few hours. The set-point temperature of the inner barrel is at room temperature rejects dissipations from payload electronics. The instrument bench runs at < 250 K and is used to maintain detector temperatures. The electronics dissipations are transported to the radiator via constant conductance heat pipes, while the detectors are sufficiently close to the radiator such that a solid-state link is used to transport waste heat.

### 4.3 Optical Configuration

The optical portion of the payload (Figure 6) comprises the telescope and instrument assembly. The instrument assembly has two main subsections: the wavefront control optics and the coronagraph. Within these two subsections, there are subassemblies that support their indicated function. The control subsection contains a fine-guidance sensor (FGS) and a Low-Order WaveFront Sensor (LOWFS) used for pointing and wavefront error correction, respectively. The final focal planes are the imager and the integral field spectrograph (IFS). The instrument assembly is located laterally with respect to the telescope axis, in a plane parallel to the telescope axis and offset to one side.

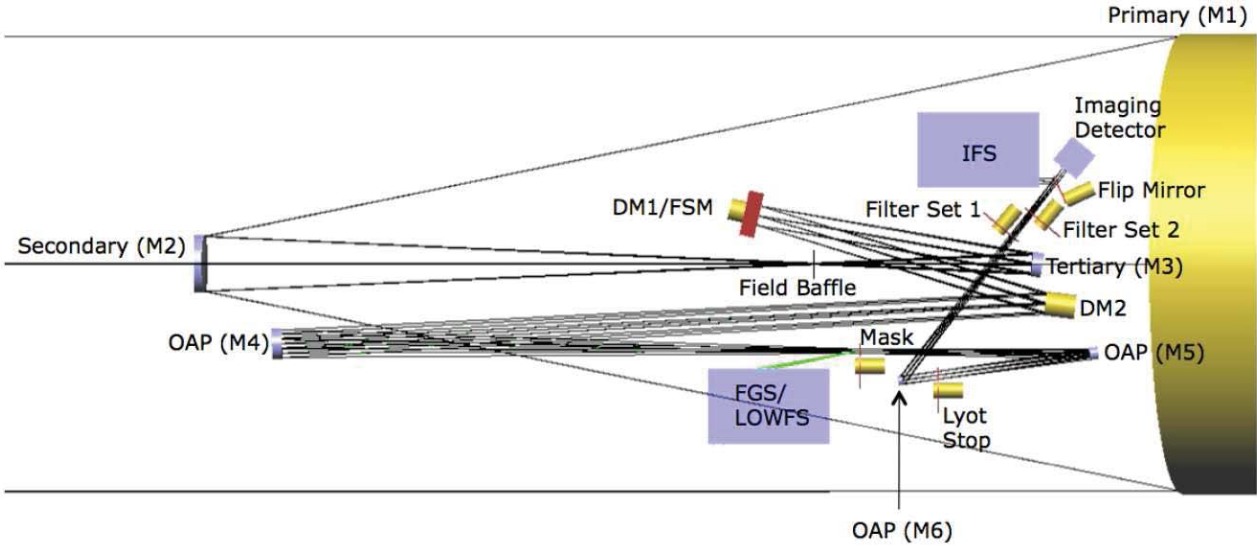


Figure 6. Baseline instrument bench layout as of the interim study report. The lateral configuration along the anti-Sun side of the telescope includes two deformable mirrors, an FGS pointing sensor, a Low-Order WaveFront Sensor (LOWFS), FSM internal pointing mechanism, coronagraphic masks & stops, spectral filters, and separate backend science camera heads for the imager and IFS.

#### 4.4 Low-order Wavefront Control

The imaging camera and the IFS are not well suited for wavefront drift measurements because the suppression of the central star means very few photons are available on these cameras. For coronagraphs employing a focal-plane mask or other optical element such as a vector vortex, it is most effective to pick up light from the central star at an image plane upstream of the focal-plane mask where photons are plentiful. This approach will be taken for both the FGS and the LOWFS. While line-of-sight error is sensed by the LOWFS, the line-of-sight drift is better handled by the dedicated FGS in a high bandwidth loop with a FSM in order to suppress not only the thermal drift of the optics but also body pointing errors and jitter. This division of function allows us to optimize the LOWFS for slowly varying WaveFront Error (WFE) terms. To sense WFE beyond the tip tilt and focus terms, it is necessary to sample the wings of the central stars PSF. A dichroic layer can be selected that reflects out-of-band light for use by the LOWFS and FGS. Our Zernike wavefront sensor version of the LOWFS has both the deformable mirror and the detector in the pupil plane so the detector is sized to match the actuator count of the deformable mirror.

#### 4.5 Spacecraft

The Exo-C spacecraft is designed to use significant Kepler heritage to meet the science requirements defined for the mission. With few exceptions, including structure, high-gain antenna (HGA), optics, and very reliable components, the spacecraft is designed to be fully redundant with all subsystems necessary to deliver the payload to orbit and support it through primary operations. The spacecraft utilizes a low-profile hexagonal box structure at the base of the coronagraph to minimize the total Flight Segment height and satisfy the fairing envelope constraints defined by intermediate class launch vehicles. The spacecraft meets all fairing volume constraints. The spacecraft utilizes a three-axis stabilized architecture, maintaining a fixed solar array pointed toward the Sun. This type of architecture minimizes jitter disturbances and shades the coronagraph telescope, helping to maintain payload thermal equilibrium. A body fixed Ka-band high-gain antenna (HGA) is used for high-rate data transmission with body-mounted X-band low-gain antennas (LGAs) for low-rate data transmission and commanding.

## 5. TECHNICAL READYNESS

Coronagraph Performance: Exo-C benefits from more than a decade of laboratory demonstrations of coronagraph performance with unobscured apertures in JPL's High Contrast Imaging Testbed (HCIT). These investments have matured the Hybrid Lyot coronagraph to a demonstrated contrast of  $1e-09$  in 20% bandwidth at  $3 \lambda/D$  inner working angle. For Exo-C, the required inner working angle is  $2 \lambda/D$ . The PIAA and Vector Vortex have demonstrated  $1e-08$  contrast performance in 10% bandwidth at  $2 \lambda/D$ . All three coronagraphs therefore require additional developments and demonstrations in the next three years in order to meet Exo-C's requirements. The AFTA/WFIRST mission study is currently investing in the Hybrid Lyot and PIAA coronagraph types, and can be expected to advance the state-of-the art in mask fabrication, apodizer fabrication, wavefront control, and system performance modeling to the benefit of Exo-C. There appears to be sufficient time and testbed access in 2016 to conduct the unobscured aperture demonstrations needed to support 2017 technical readiness.

Telescope Stability: The greatest limitation to date for the laboratory coronagraph demonstrations cited above is that they have all been done in a static instrument. The real on-orbit instrument will have its performance degraded by pointing jitter that must be actively compensated for by a fine steering mirror. In addition, thermal or vibrational disturbances are likely to cause telescope focus and alignment to slowly drift, and these need to be compensated by wavefront control adjustments during long science exposures. Telescope pointing needs to be sensed and controlled to the 1 milliarsec level at high rates, as do the contrast-degrading effects of time-variable low-order telescope aberrations. There is a need for a dynamic coronagraph performance demonstration where the needed contrast is achieved in the presence of variable pointing and low-order aberrations. The AFTA/WFIRST mission study plans to set up a new coronagraph testbed where the input stellar wavefront includes these temporal variations and where the a low-order wavefront sensor actively senses and corrects for them. This demonstration will be directly relevant to the needs of Exo-C. If successful, this would retire much of the risk of Exo-C meeting its performance requirements in a dynamic telescope environment.

Integral Field Spectrograph: Spectroscopic characterization of exoplanet atmospheres is one of the primary science goals of the mission and the integral field spectrograph (IFS) has been chosen as the most promising technology for efficient capture of the spectra. The IFS is a proven technology utilized widely on large ground-based telescopes, but the IFS has yet to be demonstrated in a flight environment. The first lenslet-based IFS was a visible-light instrument at the Canada France Hawaii Telescope (Bacon et al. 1995), and later it was proven to also be viable in the infrared with the OH-Suppressing InfraRed Imaging Spectrograph (OSIRIS) IFS at Keck (Larkin et al. 2006). Now, all of the next-generation, ground-based, high-contrast imaging systems include lenslet-based IFSs as their science cameras, therefore justifying this instrument concept at TRL 4. The only nontraditional optic in a lenslet-based IFS is the lenslet array itself. Lenslet arrays have been used to conduct science at low contrast on ground-based telescopes for the past 18 years. However, lenslet arrays need to demonstrate that they can meet the  $10^4$  spectral crosstalk requirements of a space-based high contrast imager. NASA HQ has funded a prototype IFS designed to demonstrate the needed performance (PISCES; McElwain et al. 2013), and it will be deployed to the HCIT in late 2015.

## 6. ISSUES FOR FURTHER STUDY

Cost: The Aerospace Corporation has been contracted to supply an independent Cost and Technical Evaluation (CATE) of the Exo-C concept. An initial CATE was completed in May 2014, and suggests that the interim Exo-C design exceeds the \$ 1B cost cap but by a manageable amount. Promising paths have been identified to shave down Exo-C's estimated cost and risk, and will be evaluated in follow-up CATE submissions this year and in 2015.

Kepler heritage: The Kepler photometer is exquisitely sensitive to spacecraft disturbances on its output measurements. This noise signal must be filtered out to identify planetary transits, but it contains valuable information on how well Kepler mission designers did in isolating the science instrument from disturbances and what disturbance sources might be mitigated by engineering improvements. In collaboration with the Kepler data team and Ball Aerospace engineering team, we will identify the spacecraft stability lessons to be learned from Kepler.

## 7. SUMMARY AND CONCLUSIONS

At the mid-point of the Exo-C study we have identified a mission design very similar to that of Kepler. Exo-C has virtually the same orbit, mission lifetime, telescope aperture, spacecraft and launch vehicle requirements as Kepler. Excluding reserves, its cost is expected to be comparable to that of Kepler. Additional work is being done in 2014 to lightweight and simplify the interim Exo-C design, and to better quantify its performance. At the study conclusion in early 2015, our goal is to have a compelling and viable science mission, independently costed at \$1 B or less, as a worthy successor to Kepler in the new field of exoplanet direct imaging.

The contents of this paper have been distilled from the March 2014 Exo-C Interim Study Report, CL#14-1550, available in full at [http://exep.jpl.nasa.gov/stdt/Exo-C\\_InterimReport.pdf](http://exep.jpl.nasa.gov/stdt/Exo-C_InterimReport.pdf).

## 8. REFERENCES

- Bacon, R.Y. et al. 1995, MNRAS, 326, 23
- Carlotti, A., Kasdin, N. J., Vanderbei, R. J., & Delorme, J.-R. 2012, Proc. SPIE, 8442
- Clampin, M., & Lyon, R. 2010, Pathways Towards Habitable Planets, 430, 383
- Guyon, O., Shaklan, S., Levine, M., et al. 2010, Proc. SPIE, 7731,
- Guyon, O., & Martinache, F. 2012, Proc. SPIE, 8442
- Larkin, J. et al. 2006, New Astronomy Reviews 50, 362
- Lawson, P.R. et al. 2013, Proc. SPIE, 8864
- Lyon, R. G., Clampin, M., Petrone, P., et al. 2012, Proc. SPIE, 8442
- Mawet, D., Serabyn, E., Moody, D., et al. 2011, Proc. SPIE, 8151
- McElwain, M. et al. 2013, Proc. SPIE, 8864
- Trauger, J., Stapelfeldt, K., Traub, W., et al. 2010, Proc. SPIE, 7731
- Trauger, J., Moody, D., Gordon, B., Krist, J., & Mawet, D. 2012, Proc. SPIE, 8442